

JAERI - M
86-126

RESULTS OF EDDY CURRENT TEST FOR
SECOND ROUND ROBIN BY HALDEN
REACTOR PROJECT

August 1986

Takashi IWAI, Shizuo SOUZAWA, Seiichi MIYATA
Haruyuki SAKAI and Atsushi SAKAKURA

JAERI-Mレポートは、日本原子力研究所が不定期に公刊している研究報告書です。
入手の間合わせは、日本原子力研究所技術情報部情報資料課（〒319-11茨城県那珂郡東海村）あて、お申しこしてください。なお、このほかに財団法人原子力弘済会資料センター（〒319-11茨城県那珂郡東海村日本原子力研究所内）で複写による実費頒布をおこなっております。

JAERI-M reports are issued irregularly.

Inquiries about availability of the reports should be addressed to Information Division
Department of Technical Information, Japan Atomic Energy Research Institute, Tokai-
mura, Naka-gun, Ibaraki-ken 319-11, Japan.

©Japan Atomic Energy Research Institute, 1986

編集兼発行 日本原子力研究所
印刷 いばらき印刷株式会社

Results of Eddy Current Test
for Second Round Robin by Halden
Reactor Project

Takashi IWAI, Shizuo SOUZAWA, Seiichi MIYATA,
Haruyuki SAKAI and Atsushi SAKAKURA

Department of JMTR Project,
Oarai Research Establishment,
Japan Atomic Energy Research Institute

(Received July 31, 1986)

JMTR Hot Laboratory has executed the eddy current test of two PWR type zircaloy cladding tubes for the second round robin by Halden Reactor Project.

Defects manufactured on the test specimen were revealed on a fair way to success as a function of local position, phase character and size. Influence of the fatigue crack between the two different tubes was studied through the phase angle analysis. More effort should be needed for detecting rather smaller internal defect when it was combined with external and other various type of defects.

Keywords: Eddy Current Test, Round Robin, Halden Reactor Project,
PWR Type Reactor, Zircaloy Cladding Tubes, Defect,
Fatigue Crack, JMTR Hot Laboratory

This work was conducted under the auspices of the Science and
Technology Agency of Japan.

ハルデン原子炉プロジェクトによる第2回渦電流探傷
ラウンドロビン試験の結果

日本原子力研究所大洗研究所材料試験炉部

岩井 孝・相沢 静男・宮田 精一

酒井 陽之・坂倉 敦

(1986年7月31日受理)

OECDハルデンプロジェクトにより第2回渦電流探傷ラウンドロビンが計画され、JMTRホットラボもこの計画に参加した。

ハルデンプロジェクトが準備した試料は、2本のPWRタイプのジルカロイ被覆管であり、1本は、内面及び外面欠陥、貫通ホール、リッジ等の人工欠陥を加工したキャリブレーション用であり、もう1本は、欠陥の数及び位置等が秘密の疲労クラックを加工した試験用である。

試験の結果、キャリブレーション用試料においては、ハルデンプロジェクトの情報と一致する7ヶの欠陥を検出し、試験用試料においては、13ヶの欠陥を検出し、各欠陥の位置及び大きさ等について評価することが出来た。

Contents

1. Introduction	-----	1
2. Test Apparatus	-----	1
3. Test Condition	-----	2
4. Results	-----	2
4.1 Calibration Tube	-----	3
4.1.1 Defect Location	-----	3
4.1.2 Phase Character and Defect Signal Amplitude	-----	4
4.2 Test Tube	-----	4
4.2.1 Defect Location	-----	4
4.2.2 Phase Character and Defect Signal Amplitude	-----	5
4.2.3 Defect Type and Size	-----	5
5. Conclusions	-----	5
Acknowledgment	-----	6

目 次

1. 序 言	1
2. 試 験 装 置	1
3. 試 験 条 件	2
4. 結 果	2
4.1 校正用燃料被覆管	3
4.1.1 欠陥の位置検出	3
4.1.2 欠陥信号の大きさと位相特性	4
4.2 試験用燃料被覆管	4
4.2.1 欠陥の位置検出	4
4.2.2 欠陥信号の大きさと位相特性	5
4.2.3 欠陥の型と大きさ	5
5. 結 論	5
謝 辞	6

1. INTRODUCTION

The second round robin for eddy current test initiated from April, 1985, in accordance with the recommendation of workshop meeting held at the Halden in Norway in March, 1983, on the result^{1),2)} of the first round robin eddy current test performed during years 1981 to 1982. JMTR Hot Laboratory, Oarai Research Establishment, JAERI also participated to this programme. Test execution of JAERI was March, 1986.

Received test tube had a length of 1,000 mm, outer diameter of 10.93 mm, wall thickness of 0.63 mm. On the other hand, calibration tube had a length of 1,000 mm, outer diameter of 10.93 mm, wall thickness of 0.625 mm.

Principal purpose of this round robin test is for determining the criteria of detectable crack through eddy current test. Our test apparatus were now renewed in 1984. They have two detection coils consist of encircling and probe types. This apparatus permits not only to measure a various type of defects but to detect, for example, a thickness of oxide layer and copper barrier. The former function is utilized this eddy current test.

2. TEST APPARATUS

The apparatus was the EDDIO SORT FD-2203 NGO-R manufactured by HARA Electronics Co. Ltd., Tokyo, Japan. This consists of a detection coil device fitted up with an encircling and a probe coil, and a sample moving device installed inside of the hot cell. A control panel and a data processing unit are located outside of the hot cell. The outline of the apparatus is shown in Fig. 1. A sample tube is held in vertical manner by the chuck mechanism and moved through the coil keeping the tube center with the guide roller. During the test, the sample usually moved upward. The move was monitored by the pulse-encoder. The scanning speed can varied in the range of 5 to 30 mm/sec. For azimuthal measurement, the sample tube can rotate in continuous or step manner. The intervals at step manner can varied from 10 to 90 degree. For specified scanning by the probe coil, the azimuth of sample tube can selectable with an interval of 1 degree.

Encircling and probe coils are shown in Fig. 2. They consisted of two pick-up coils and an exciting one. The coils are copper wire coated with

1. INTRODUCTION

The second round robin for eddy current test initiated from April, 1985, in accordance with the recommendation of workshop meeting held at the Halden in Norway in March, 1983, on the result^{1),2)} of the first round robin eddy current test performed during years 1981 to 1982. JMTR Hot Laboratory, Oarai Research Establishment, JAERI also participated to this programme. Test execution of JAERI was March, 1986.

Received test tube had a length of 1,000 mm, outer diameter of 10.93 mm, wall thickness of 0.63 mm. On the other hand, calibration tube had a length of 1,000 mm, outer diameter of 10.93 mm, wall thickness of 0.625 mm.

Principal purpose of this round robin test is for determining the criteria of detectable crack through eddy current test. Our test apparatus were now renewed in 1984. They have two detection coils consist of encircling and probe types. This apparatus permits not only to measure a various type of defects but to detect, for example, a thickness of oxide layer and copper barrier. The former function is utilized this eddy current test.

2. TEST APPARATUS

The apparatus was the EDDIO SORT FD-2203 NGO-R manufactured by HARA Electronics Co. Ltd., Tokyo, Japan. This consists of a detection coil device fitted up with an encircling and a probe coil, and a sample moving device installed inside of the hot cell. A control panel and a data processing unit are located outside of the hot cell. The outline of the apparatus is shown in Fig. 1. A sample tube is held in vertical manner by the chuck mechanism and moved through the coil keeping the tube center with the guide roller. During the test, the sample usually moved upward. The move was monitored by the pulse-encoder. The scanning speed can varied in the range of 5 to 30 mm/sec. For azimuthal measurement, the sample tube can rotate in continuous or step manner. The intervals at step manner can varied from 10 to 90 degree. For specified scanning by the probe coil, the azimuth of sample tube can selectable with an interval of 1 degree.

Encircling and probe coils are shown in Fig. 2. They consisted of two pick-up coils and an exciting one. The coils are copper wire coated with

enamel. The wire diameter of encircling coil was 0.1 mm and 0.26 mm for pick-up and exciting coil. On the other hand, wire diameter of the probe coil was 0.05 mm and 0.08 mm for pick-up coil and exciting one.

The encircling coil was used to detect the type, size, and axial position of exciting defects. While, the probe coil was used to detect the azimuthal position of local defects.

Data processing unit was composed of an oscillograph to record the analog data, a set of personal computer system together with A/D converter and digital data recorder, and a X-Y plotter. The digitalized data from the probe coil could make three-dimensional plotting which was easy to observe the being defects. On the other hand, test signals of encircling coils could characterize the phase angle and the amplitude.

3. TEST CONDITION

The test apparatus with dual frequency type could perform two kinds of scanning simultaneously at selected two frequency levels so that the following sets of test frequencies were used: 16, 32, 64, 128 kHz and 128, 256, 512, 1024 kHz.

Calibration test with the calibration tube was performed. The outline of the calibration tube is shown in Fig. 3. It was aimed at determining the suitable condition for the detection of artificial defects such as internal, external, through hole, ridge and so on. Test conditions were:

(a) Test frequency:

Channel 1	64 kHz,	128 kHz
Channel 2	256 kHz,	512 kHz

(b) Scanning velocity: 20 mm/sec, 30 mm/sec

(c) Band-pass filter adjustment:

low pass filter	10 to 30 Hz
high pass filter	2 to 10 Hz

Final conditions decided from the above were:

(a) Coil exciting frequency:

Channel 1	64 kHz
Channel 2	256 kHz

(b) Scanning velocity: 20 mm/sec

(c) Band-pass filter: 4 to 20 Hz

4. RESULTS

enamel. The wire diameter of encircling coil was 0.1 mm and 0.26 mm for pick-up and exciting coil. On the other hand, wire diameter of the probe coil was 0.05 mm and 0.08 mm for pick-up coil and exciting one.

The encircling coil was used to detect the type, size, and axial position of exciting defects. While, the probe coil was used to detect the azimuthal position of local defects.

Data processing unit was composed of an oscillograph to record the analog data, a set of personal computer system together with A/D converter and digital data recorder, and a X-Y plotter. The digitalized data from the probe coil could make three-dimensional plotting which was easy to observe the being defects. On the other hand, test signals of encircling coils could characterize the phase angle and the amplitude.

3. TEST CONDITION

The test apparatus with dual frequency type could perform two kinds of scanning simultaneously at selected two frequency levels so that the following sets of test frequencies were used: 16, 32, 64, 128 kHz and 128, 256, 512, 1024 kHz.

Calibration test with the calibration tube was performed. The outline of the calibration tube is shown in Fig. 3. It was aimed at determining the suitable condition for the detection of artificial defects such as internal, external, through hole, ridge and so on. Test conditions were:

(a) Test frequency:

Channel 1	64 kHz,	128 kHz
Channel 2	256 kHz,	512 kHz

(b) Scanning velocity: 20 mm/sec, 30 mm/sec

(c) Band-pass filter adjustment:

low pass filter	10 to 30 Hz
high pass filter	2 to 10 Hz

Final conditions decided from the above were:

(a) Coil exciting frequency:

Channel 1	64 kHz
Channel 2	256 kHz

(b) Scanning velocity: 20 mm/sec

(c) Band-pass filter: .4 to 20 Hz

4. RESULTS

enamel. The wire diameter of encircling coil was 0.1 mm and 0.26 mm for pick-up and exciting coil. On the other hand, wire diameter of the probe coil was 0.05 mm and 0.08 mm for pick-up coil and exciting one.

The encircling coil was used to detect the type, size, and axial position of exciting defects. While, the probe coil was used to detect the azimuthal position of local defects.

Data processing unit was composed of an oscillograph to record the analog data, a set of personal computer system together with A/D converter and digital data recorder, and a X-Y plotter. The digitalized data from the probe coil could make three-dimensional plotting which was easy to observe the being defects. On the other hand, test signals of encircling coils could characterize the phase angle and the amplitude.

3. TEST CONDITION

The test apparatus with dual frequency type could perform two kinds of scanning simultaneously at selected two frequency levels so that the following sets of test frequencies were used: 16, 32, 64, 128 kHz and 128, 256, 512, 1024 kHz.

Calibration test with the calibration tube was performed. The outline of the calibration tube is shown in Fig. 3. It was aimed at determining the suitable condition for the detection of artificial defects such as internal, external, through hole, ridge and so on. Test conditions were:

(a) Test frequency:

Channel 1	64 kHz,	128 kHz
Channel 2	256 kHz,	512 kHz

(b) Scanning velocity: 20 mm/sec, 30 mm/sec

(c) Band-pass filter adjustment:

low pass filter	10 to 30 Hz
high pass filter	2 to 10 Hz

Final conditions decided from the above were:

(a) Coil exciting frequency:

Channel 1	64 kHz
Channel 2	256 kHz

(b) Scanning velocity: 20 mm/sec

(c) Band-pass filter: .4 to 20 Hz

4. RESULTS

4.1. CALIBRATION TUBE

Phase angle and amplitude were tried to characterize the being artificial defect. Due to little difference between data obtained from frequency 64 kHz and from frequency 256 kHz, results were only addressed to the latter.

4.1.1. DEFECT LOCATION

Fig. 4 shows representative output chart for the calibration test with the encircling coil. Defect signals and positions are included in it. Fig. 5 shows three-dimensional plotting of defect signals obtained from the probe coil. Axial and azimuthal position of the defects are clearly and detaily shown. Table 1 indicates the results of azimuth, size and type of defects evaluated from Figs. 4 and 5.

Consequently, the defects noted in Table 1 well coincided with those noted in Fig. 3. The details on latter were given by the Halden Reactor Project.

Signal from defect No. ⑦ was not enough to make detail analysis. One of main reason was that the signal obtained from probe coil was too weak. It should be mentioned that the surface condition and the residual stress uniformity in the place were bad. It was supposed that the tubes were pre-stressed in defect-manufacturing process and unintentionally added small defects when they were tested in a participant facility.

In Fig. 5, no signal was observed at the position of 950 mm, 0° but some signal did at the 950 mm, 130° direction. According to our evaluation, this was an external defect which was different from Halden informed defect type (No. ⑦ : internal scar). Amplifier gain was then increased at the place for detecting the signal at 950 mm, 5° direction. The result of the gain increment analysis was included in Table 1.

It was understood from the test with probe coil (see Fig. 5) that defect signals of Nos. ④, ⑤ and ⑥ were respectively within a width of 70°, 50° and 60° in azimuth. These widths were resulted in good agreement with calculations made by using the probe coil diameter (2.5 mm), the tube outer diameter (10.92 mm) and the Halden informed defect diametral sizes (1.0, 0.2, 0.5 mm).

4.1.2. PHASE CHARACTER AND DEFECT SIGNAL AMPLITUDE

As shown in Figs. 6 to 8, analysis of signal amplitude and phase angle on the calibration tube was made. Results are shown in Table 1. Characterized phase angle is indicated in Fig. 20. In the figure, the Halden made defects were located at the region: 1) 65° to 70°, 2) 40°, 3) 50° to 55° and 4) 275° being corresponded to 1) external, 2) internal, 3) through hole and 4) ridge. The calibration curves were made from the signal amplitude and defect size which were shown in Table 1. Results are summed up in Figs. 9 to 12. In which four different curves are shown, i.e. internal defects (Nos. ① and ⑦), external defect (No. ④), through hole (Nos. ⑤ and ⑥) and ridge (No. ②), respectively.

4.2. TEST TUBE

With aid of preliminary test result obtained from the calibration tube, type and size of defects on the test tube were evaluated. The frequency used here was similar to that used in the previous test, i.e. 256 kHz.

4.2.1. DEFECT LOCATION

Obtained output chart from the encircling coil test is shown in Fig. 13 in which axial position of each defect is involved. Fig. 14 shows three dimensional plotting of obtained signals from probe coil scan. Defect position in axial and azimuthal directions are also shown in the figure. Table 2 summed up obtained results from the analysis of Figs. 13 and 14.

Data evaluation was limited only on defect Nos. (a) to (m). Those were existed within 600 mm in length which was apated 200 mm from tube both ends. The surface condition in this time was also bad as the same reason as mentioned previously. The worst was length 200 mm around bottom end.

As shown in Fig. 14, all defects were adequately distributed on the whole surface of tube, and detected azimuthal range of 50° to 60°. In Fig. 14, defect signals from Nos. (f) to (g) and No. (k) were too small to discriminate, then azimuthal position of them were asked to determine by additional output chart obtained from a specially-amplified signal. Results of defect characterization are shown in Table 2.

4.2.2. PHASE CHARACTER AND DEFECT SIGNAL AMPLITUDE

Analyzed phase angles are shown in Figs. 15 to 19. Table 2 is the summary. The phase angles from the test and the calibration tube were plotted in Fig. 20. As known from Fig. 20, test tube signals Nos. (a) to (d) (phase angle: 50-55°) coincided with through hole (calibration signals Nos. (5) to (6)). On the other hand, signal No. (i) (phase angle: 260°) coincided with ridge (calibration signals No. (2)). The remainders (phase angle: 80-130°), however, had no good correspondence.

Our experience²⁾ led that the phase angle deviation between fatigue cracks and other type of defects were approximately 10 to 20°.

4.2.3. DEFECT TYPE AND SIZE

It can be mentioned from Fig. 20 that the phase angle was representing the fatigue crack. According to this, it could be said that signals from Nos. (a) to (d) were internal type and those from Nos. (e) to (m) external type defects.

The defect volume was summarized in Table 2, in which the calibration results from Fig. 9 for signals Nos. (a) to (d) and Fig. 10 for those Nos. (e) to (m) were used.

It was assumed that the defect was composed of 2 mm length, 0.5 mm width and unknown depth. Estimated defect depth by using Table 2 was 0.28 to 0.36 mm for defects Nos. (a) to (d) and 0.01 to 0.03 mm for those Nos. (e) to (m). Because of little necessary data for determining defect size and type, it was a little room for mentioning about them. Thus, defects Nos. (e) to (m) could be divided into three groups.

First group including defects Nos. (e), (h), (j), (l) and (m) was called the "internal and external defects combined with unintentional noise". Second group including defects Nos. (f), (g) and (k) was called the "external defects combined with unintentional noise". Last group including defect No. (i) was called the "masked defect like ridge".

5. CONCLUSIONS

JMTR Hot Laboratory performed the eddy current test for the second round robin programme. Obtained concluding remarks are:

4.2.2. PHASE CHARACTER AND DEFECT SIGNAL AMPLITUDE

Analyzed phase angles are shown in Figs. 15 to 19. Table 2 is the summary. The phase angles from the test and the calibration tube were plotted in Fig. 20. As known from Fig. 20, test tube signals Nos. (a) to (d) (phase angle: 50-55°) coincided with through hole (calibration signals Nos. (5) to (6)). On the other hand, signal No. (i) (phase angle: 260°) coincided with ridge (calibration signals No. (2)). The remainders (phase angle: 80-130°), however, had no good correspondence.

Our experience²⁾ led that the phase angle deviation between fatigue cracks and other type of defects were approximately 10 to 20°.

4.2.3. DEFECT TYPE AND SIZE

It can be mentioned from Fig. 20 that the phase angle was representing the fatigue crack. According to this, it could be said that signals from Nos. (a) to (d) were internal type and those from Nos. (e) to (m) external type defects.

The defect volume was summarized in Table 2, in which the calibration results from Fig. 9 for signals Nos. (a) to (d) and Fig. 10 for those Nos. (e) to (m) were used.

It was assumed that the defect was composed of 2 mm length, 0.5 mm width and unknown depth. Estimated defect depth by using Table 2 was 0.28 to 0.36 mm for defects Nos. (a) to (d) and 0.01 to 0.03 mm for those Nos. (e) to (m). Because of little necessary data for determining defect size and type, it was a little room for mentioning about them. Thus, defects Nos. (e) to (m) could be divided into three groups.

First group including defects Nos. (e), (h), (j), (l) and (m) was called the "internal and external defects combined with unintentional noise". Second group including defects Nos. (f), (g) and (k) was called the "external defects combined with unintentional noise". Last group including defect No. (i) was called the "masked defect like ridge".

5. CONCLUSIONS

JMTR Hot Laboratory performed the eddy current test for the second round robin programme. Obtained concluding remarks are:

- 1) Seven and thirteen defects for the calibration and the test tube were revealed as a function of position, phase character and size.
- 2) Among thirteen defects on test tube, four of which were clearly identified as the internal defects and the remainders were as external ones.
- 3) The phase angle on the test tube was deviated a little from that on the calibration tube, implying the rather strong influence of fatigue crack on phase angle.
- 4) Greater noise occurred from non-smooth tube surface tended to mask the existing defects. The influence was particularly greater when the evaluation was made on the internal defects.
- 5) At present, it was very hard to detect markedly small internal defect for the purpose of evaluating its phase character and size. The difficulty will be more enhanced when smaller internal defect is combined with external or other type of defects.

ACKNOWLEDGMENT

The authors wish to express their thanks to Dr.Y.Okamoto, Director of Department of JMTR Project, for his encouragement, and also to Dr.S.Kawasaki, Head of Fuel Reliability Laboratory III, Department of Fuel Safety Research, for their arrangement. Their thanks are also due to colleagues in Hot Laboratory, Department of JMTR Project, for their cooperation.

REFERENCES

- 1) E.Patrakka and R.J.P.Cribb: Report of the workshop meeting on eddy-current testing of Zircaloy tubes (Round-robin exercise), HWR-91, May 1983.
- 2) T.Iwai et al.: Results of eddy-current test on Zircaloy tubes (Round-robin exercise arranged by OECD Halden Reactor Project), Feb. 1984.

- 1) Seven and thirteen defects for the calibration and the test tube were revealed as a function of position, phase character and size.
- 2) Among thirteen defects on test tube, four of which were clearly identified as the internal defects and the remainders were as external ones.
- 3) The phase angle on the test tube was deviated a little from that on the calibration tube, implying the rather strong influence of fatigue crack on phase angle.
- 4) Greater noise occurred from non-smooth tube surface tended to mask the existing defects. The influence was particularly greater when the evaluation was made on the internal defects.
- 5) At present, it was very hard to detect markedly small internal defect for the purpose of evaluating its phase character and size. The difficulty will be more enhanced when smaller internal defect is combined with external or other type of defects.

ACKNOWLEDGMENT

The authors wish to express their thanks to Dr.Y.Okamoto, Director of Department of JMTR Project, for his encouragement, and also to Dr.S.Kawasaki, Head of Fuel Reliability Laboratory III, Department of Fuel Safety Research, for their arrangement. Their thanks are also due to colleagues in Hot Laboratory, Department of JMTR Project, for their cooperation.

REFERENCES

- 1) E.Patrakka and R.J.P.Cribb: Report of the workshop meeting on eddy-current testing of Zircaloy tubes (Round-robin exercise), HWR-91, May 1983.
- 2) T.Iwai et al.: Results of eddy-current test on Zircaloy tubes (Round-robin exercise arranged by OECD Halden Reactor Project), Feb. 1984.

Table. 1 RESULT OF EDDY CURRENT TEST ON CALIBRATION TUBE

Defect No.	Position		Size	Type	Phase angle (°)	Signal amplitude (V)
	Axial (mm) ※1	Azimuthal (°) ※2				
①	50	0~360	0.31 (mm ³)	Internal defect	40	0.92
②	200	0~360	40 (μm)	Ridge	275	17.81
③a	340	0~360	34.3 (mm ³)	External defect	70	22.90
③b	360				250	26.78
④	500	0	0.16 (mm ³)	External defect	65	3.56
⑤	650	10	φ0.2 (mm)	Through hole	55	0.53
⑥	800	10	φ0.5 (mm)	∕	50	2.47
⑦	950	5	0.14 (mm ³)	Internal defect	40	0.07

※1. Distance from the top end to defect center.

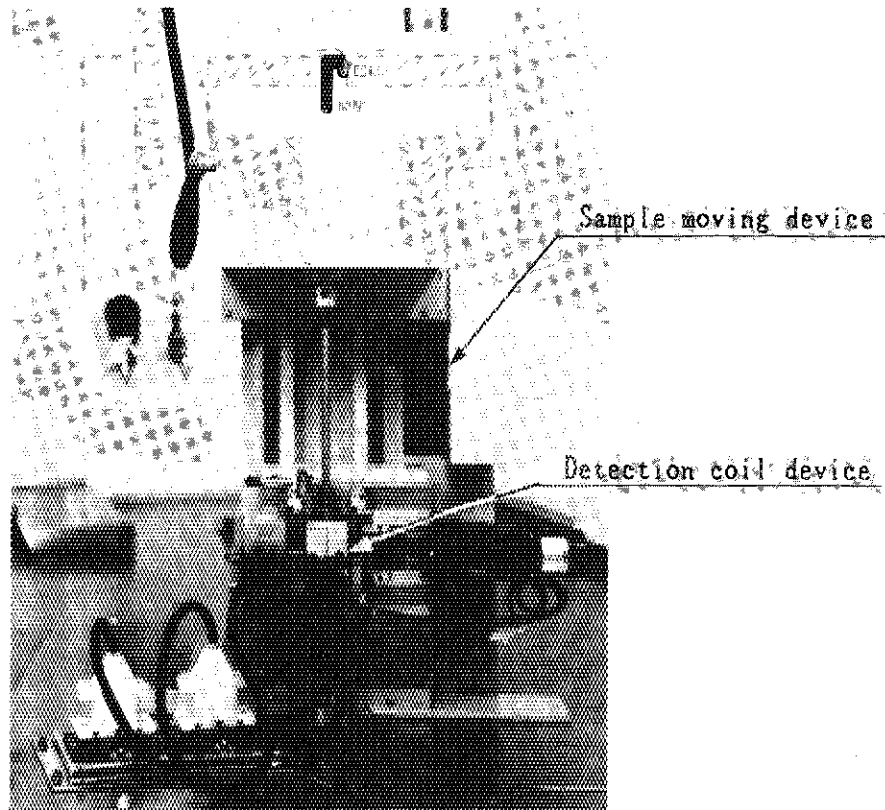
※2. Clock wise degree from the oriental mark to defect center.

Table. 2 CHARACTERIZATION OF TEST TUBE DEFECTS

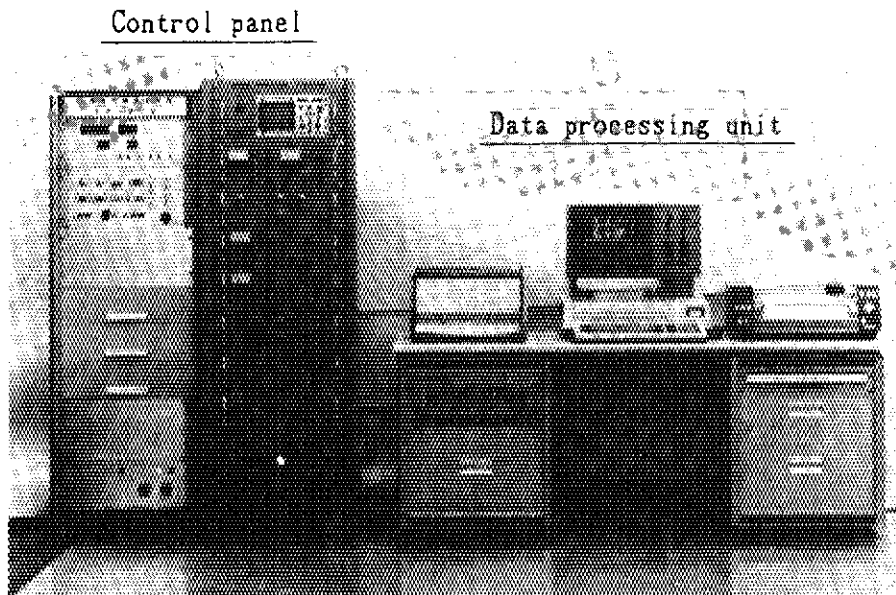
Defect No.	Position		Phase angle (°)	Type	Signal amplitude (V)	Volume (mm ³)
	Axial (mm) ※1	Azimuthal (°) ※2				
(a)	206	~265	50	Internal	1.50	0.36
(b)	333	~170	50	"	0.78	0.29
(c)	432	~75	55	"	0.96	0.32
(d)	506	~335	55	"	0.66	0.28
(e)	577	~205	90	External	0.41	0.03
(f)	595	~130	80	"	0.34	0.02
(g)	617	~45	80	"	0.24	0.02
(h)	637	~135	80	"	0.25	0.02
(i)	665	~140	260	"	0.36	0.03
(j)	697	~295	130	"	0.11	0.01
(k)	726	~35	80	"	0.25	0.02
(l)	753	~60	120	"	0.29	0.02
(m)	802	~0	110	"	0.30	0.02

※1. Distance from the top end to defect center.

※2. Clock wise degree from the oriental mark to defect center.



IN-CELL DEVICE



OUT-CELL UNITS

Fig. 1 OUTLINE OF EDDY CURRENT TEST APPARATUS

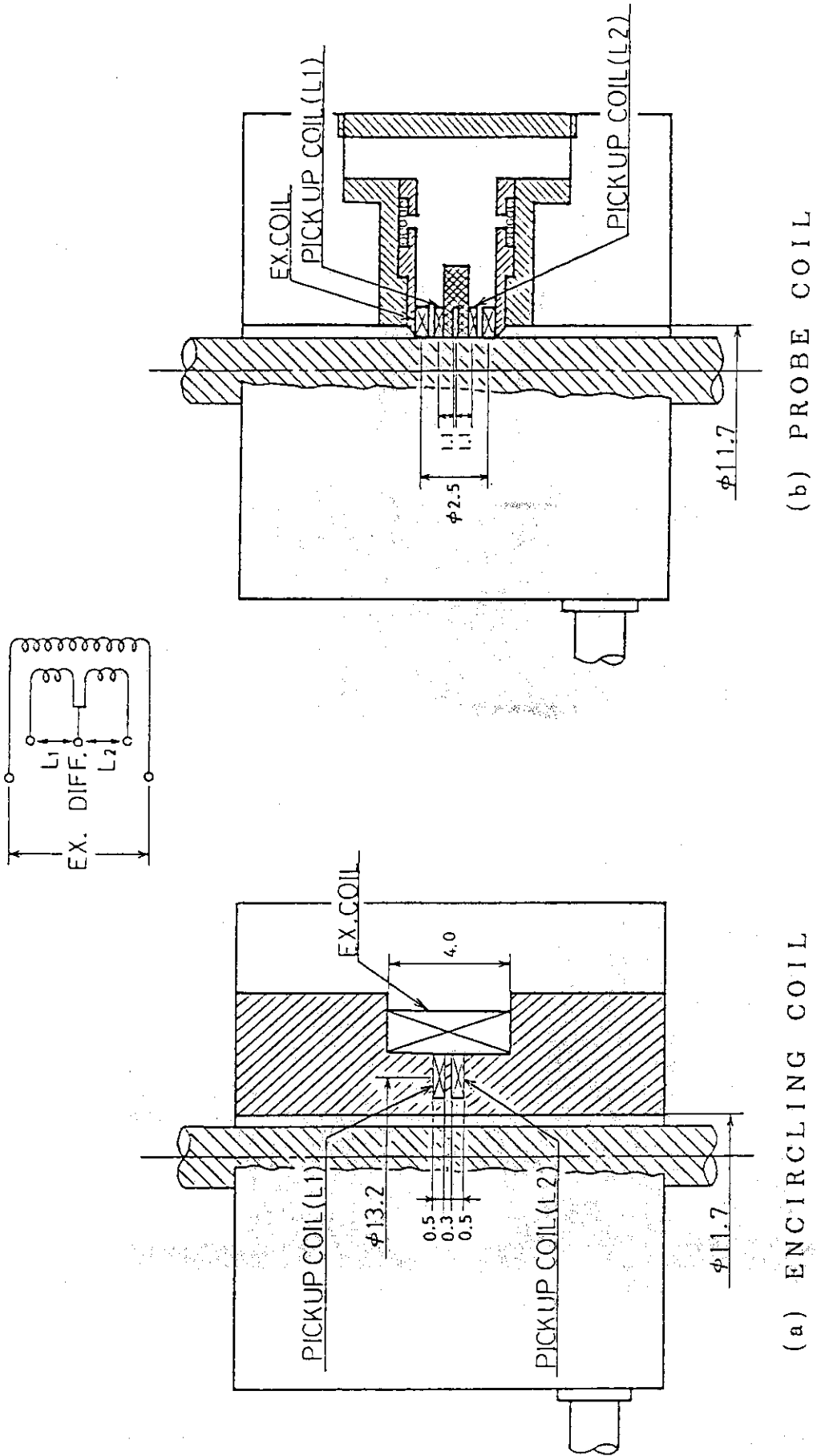
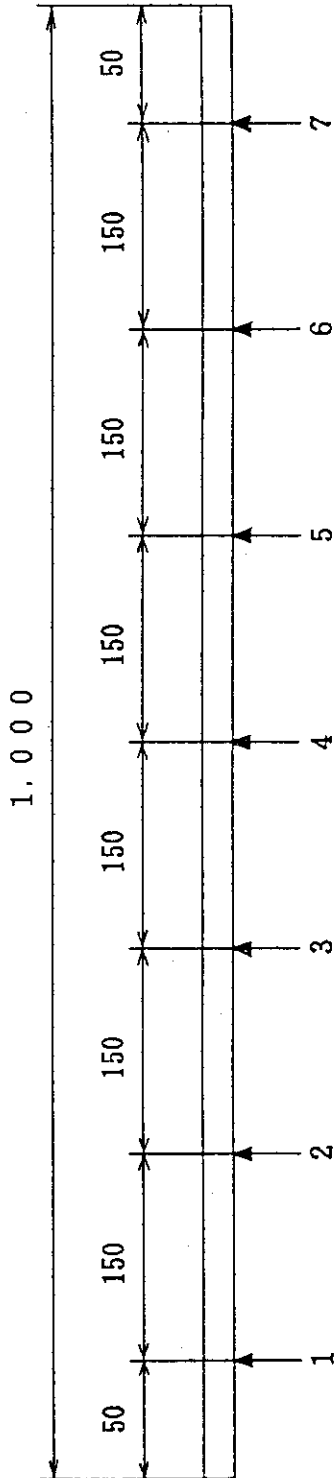


Fig. 2 EDDY CURRENT COIL



Defect No.	Type	Dimension
1	Internal groove	0.1 × 0.1 (Circular)
2	External ridge	40 (μm)
3	External reduced wall	20 × 0.05
4 ※	External scar (Blind hole nearly flat bottomed)	φ 1 × 0.2
5 ※	Through hole	φ 0.2
6 ※	"	φ 0.5
7 ※	Internal scar	1 × 0.7 × 0.2 (1 × w × d)

※ On line with orient mark on end of tube.

Fig. 3 OUTLINE OF THE CALIBRATION TUBE

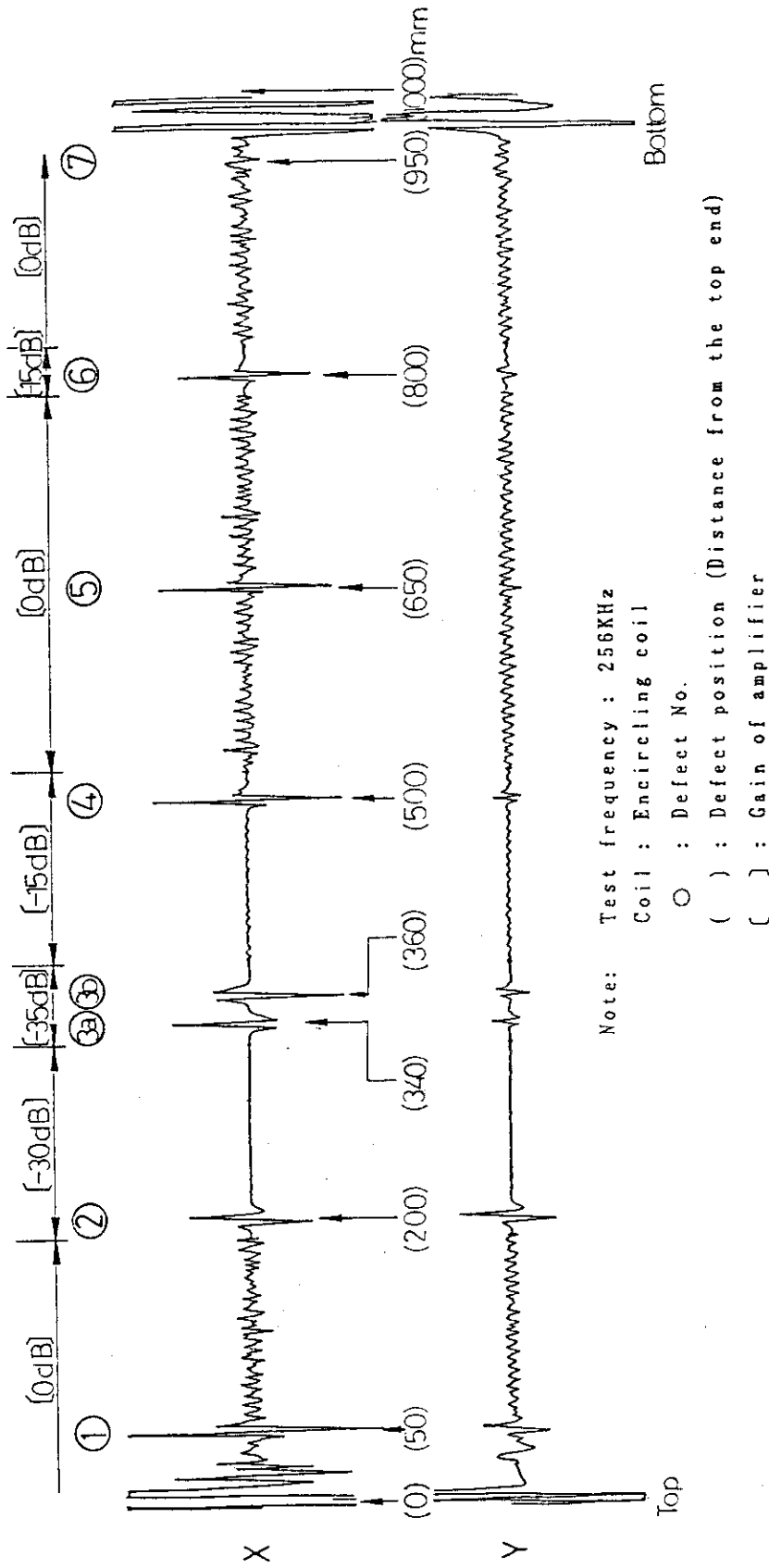


Fig. 4 REPRESENTATIVE OUTPUT CHART ON CALIBRATION TUBE

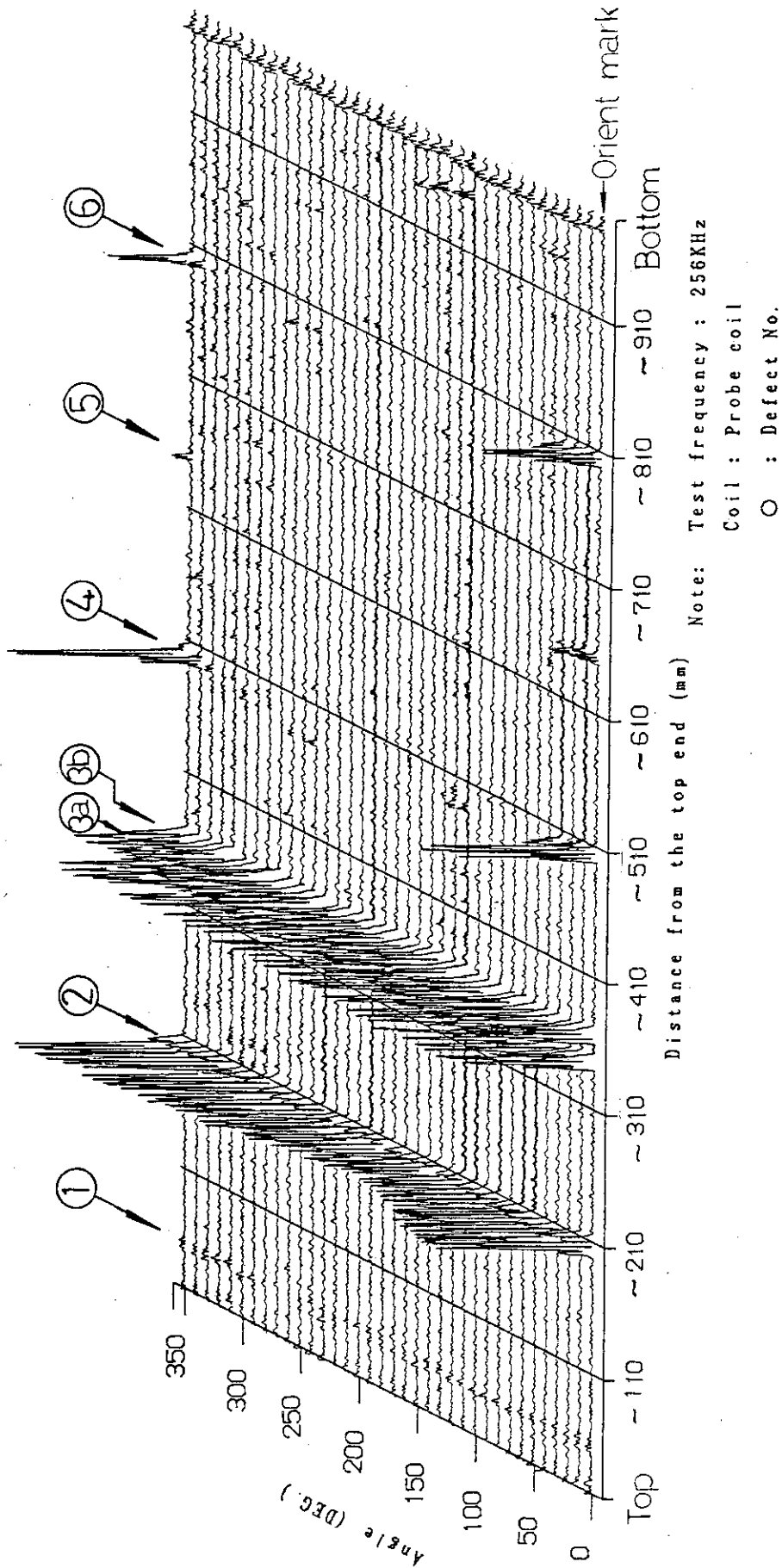
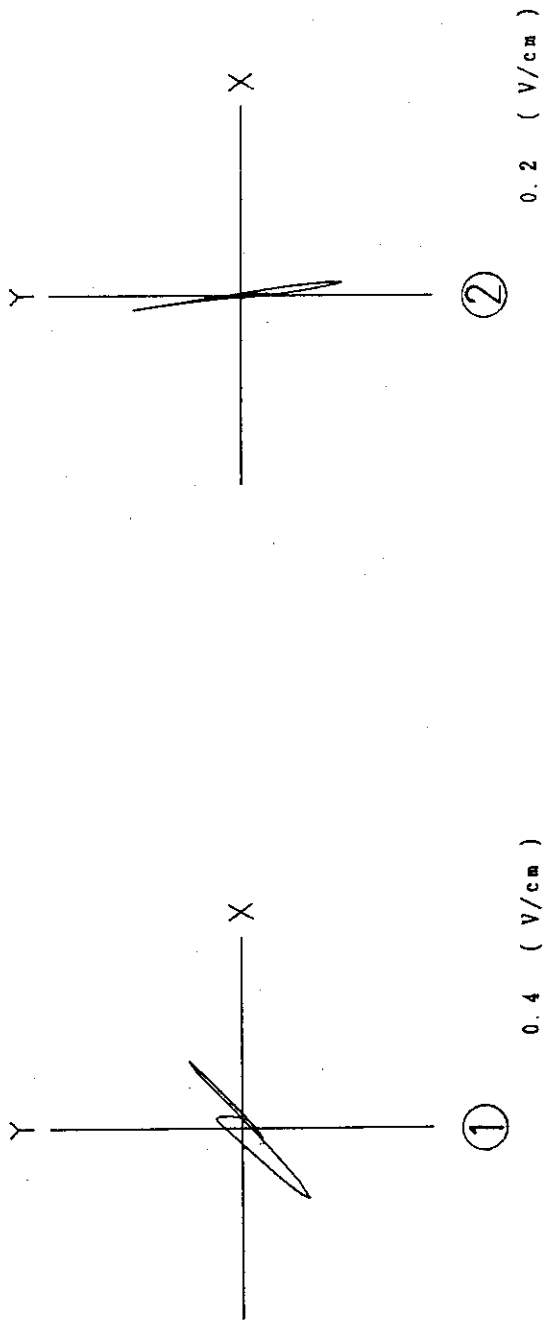
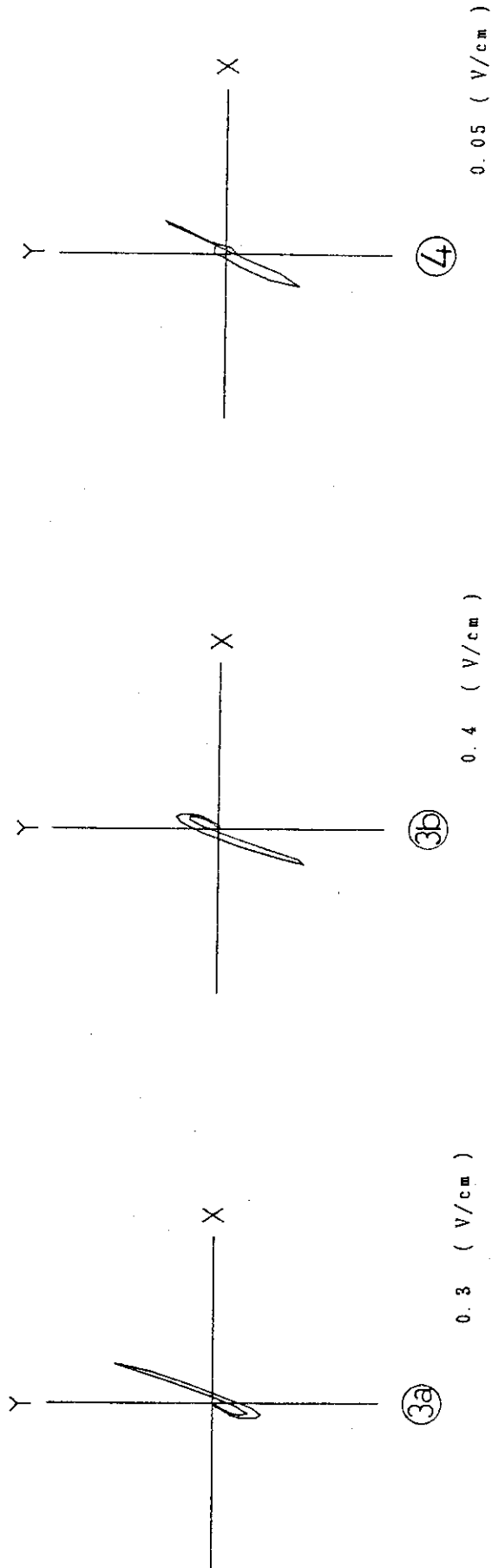


Fig. 5 THREE DIMENSIONAL PLOTS OF SIGNALS FOR CALIBRATION TUBE



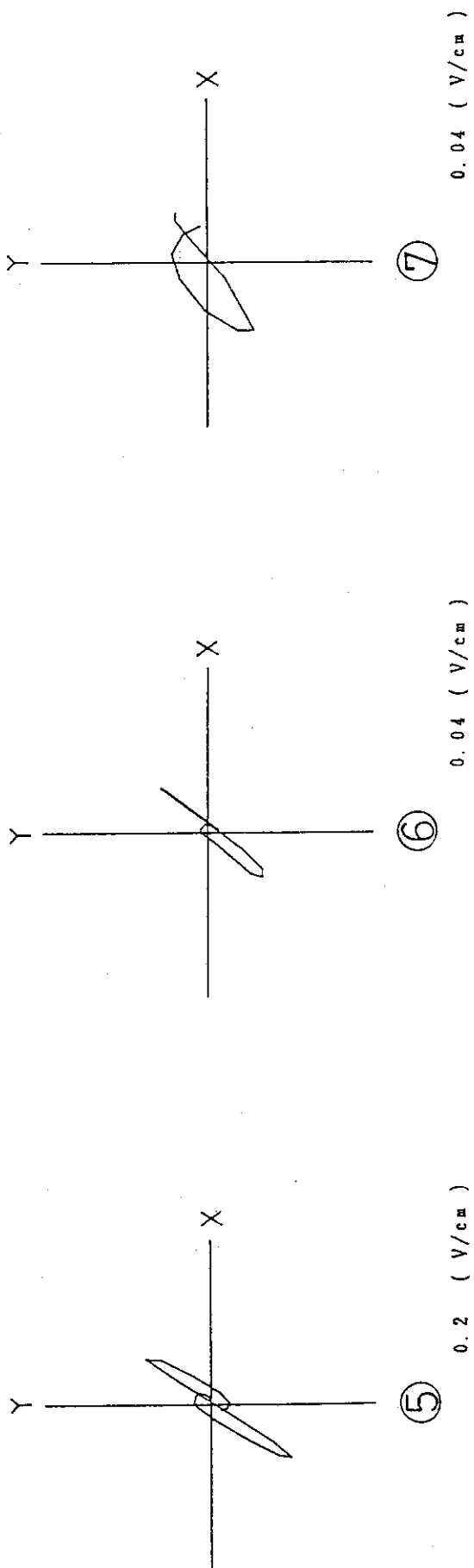
Note: Test frequency: 256KHz
Coil: Encircling coil

Fig. 6 X-Y PLOTS FOR DEFECT No. ①, ② IN CALIBRATION TUBE



Note: Test frequency: 256KHz
Coil: Encircling coil

Fig. 7 X-Y PLOTS FOR DEFECT No. 3a, 3b, 4 IN CALIBRATION TUBE



Note: Test frequency: 256KHz
Coil : Encircling coil

Fig. 8 X-Y PLOTS FOR DEFECT No. ⑤, ⑥, ⑦ IN CALIBRATION TUBE

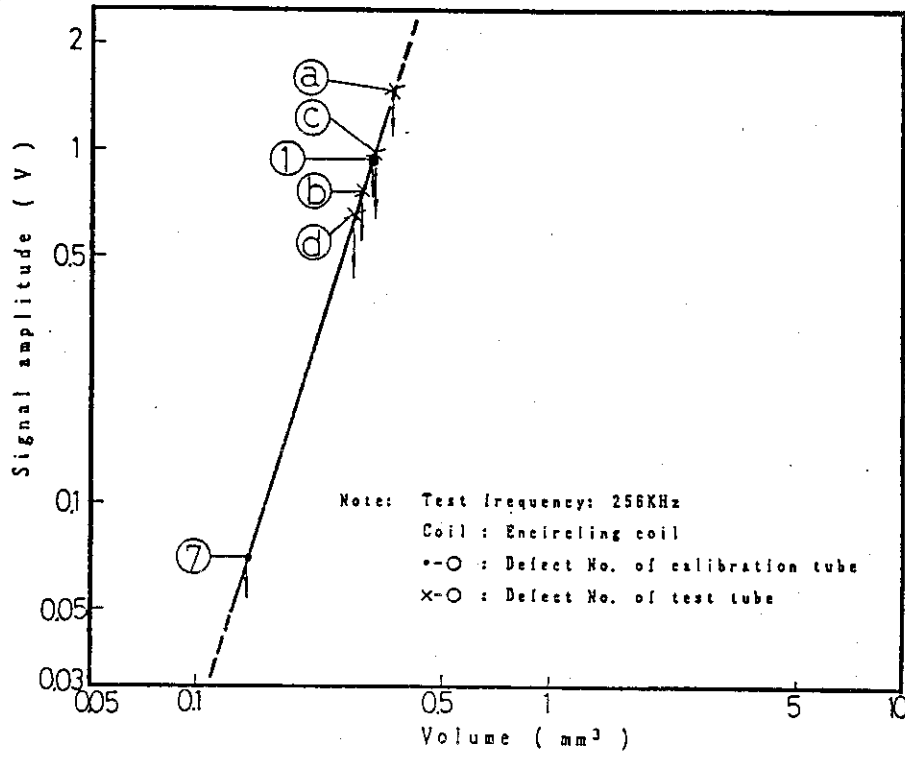


Fig. 9 CALIBRATION CURVE FOR INTERNAL DEFECTS

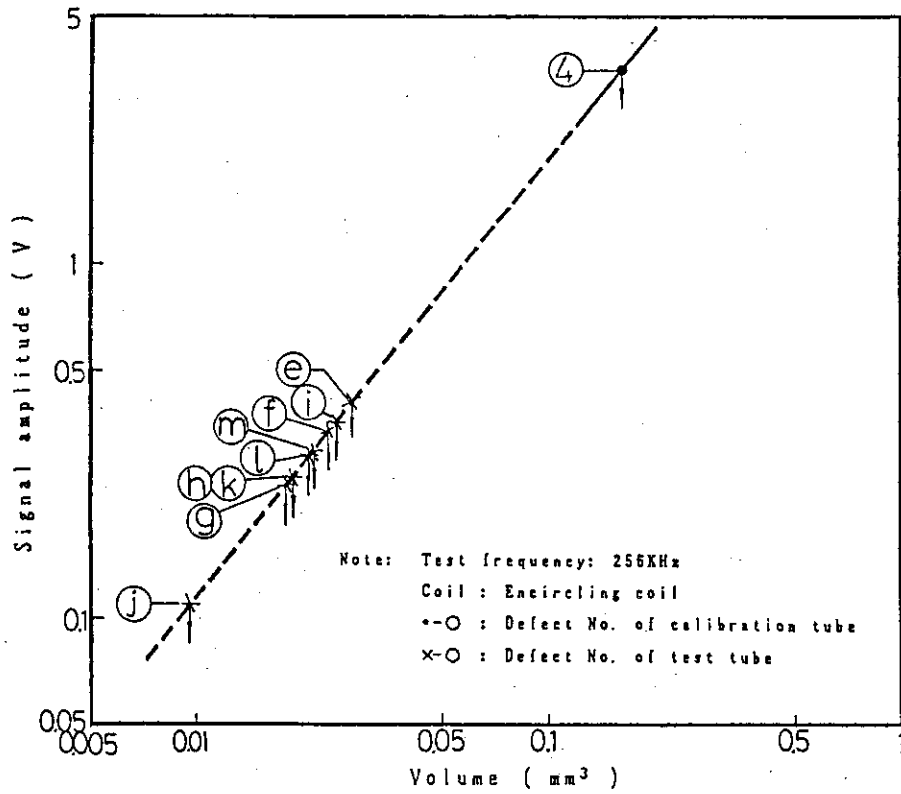


Fig. 10 CALIBRATION CURVE FOR EXTERNAL DEFECTS

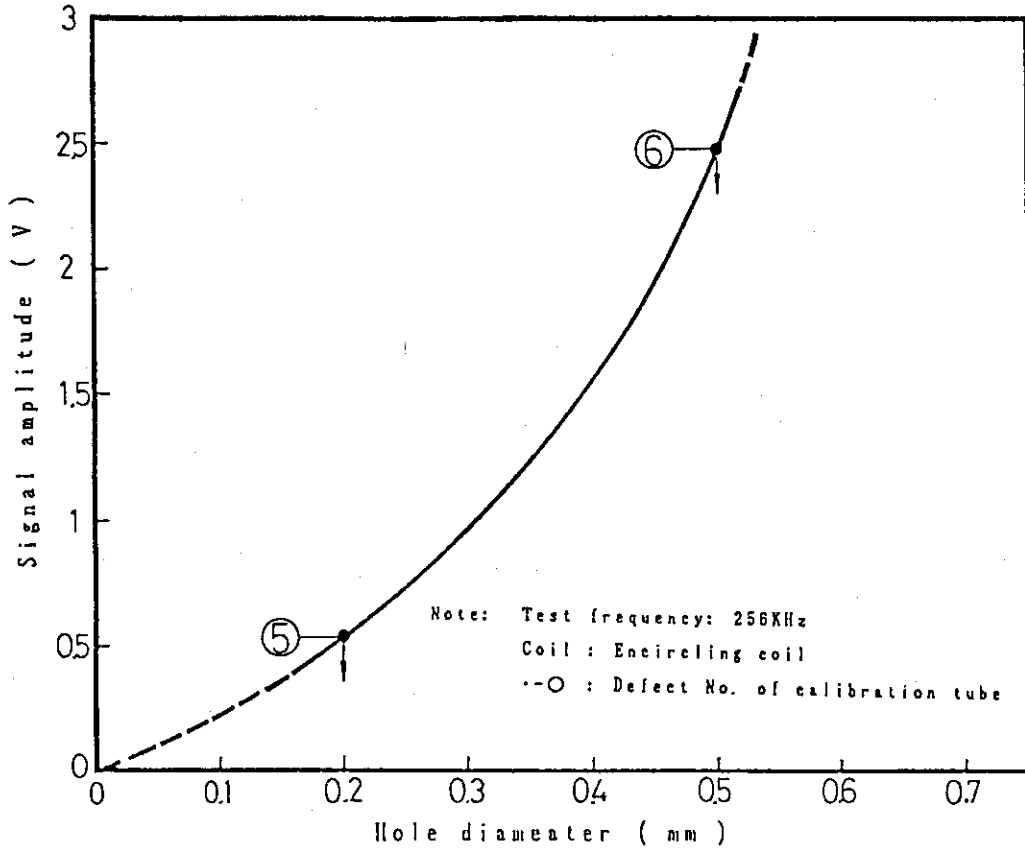


Fig. 11 CALIBRATION CURVE FOR THROUGH HOLE

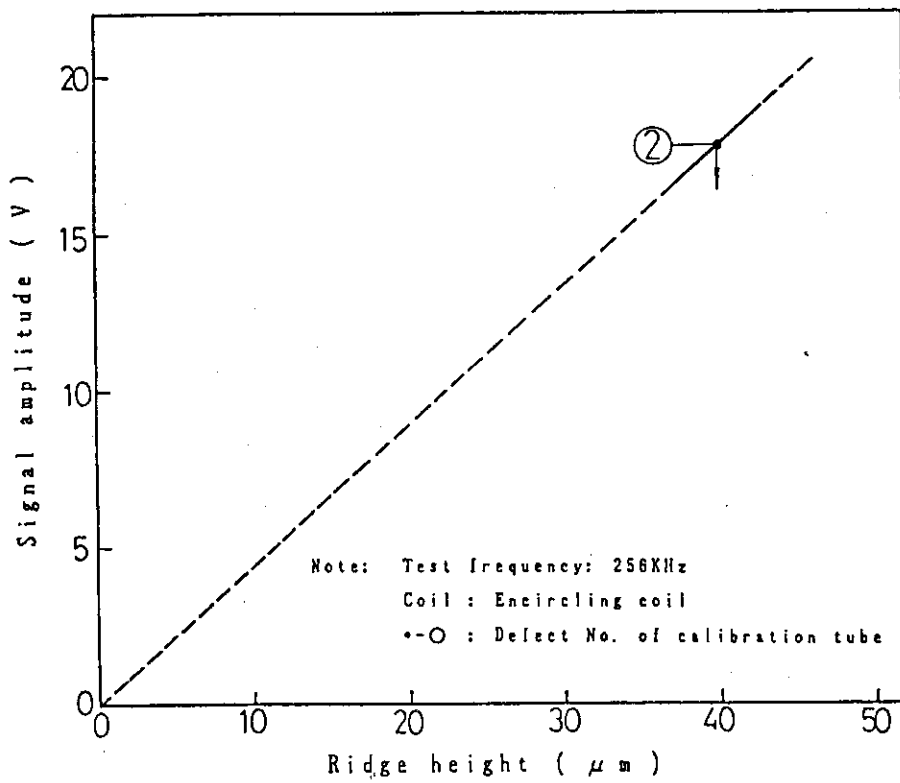


Fig. 12 CALIBRATION CURVE FOR RIDGE

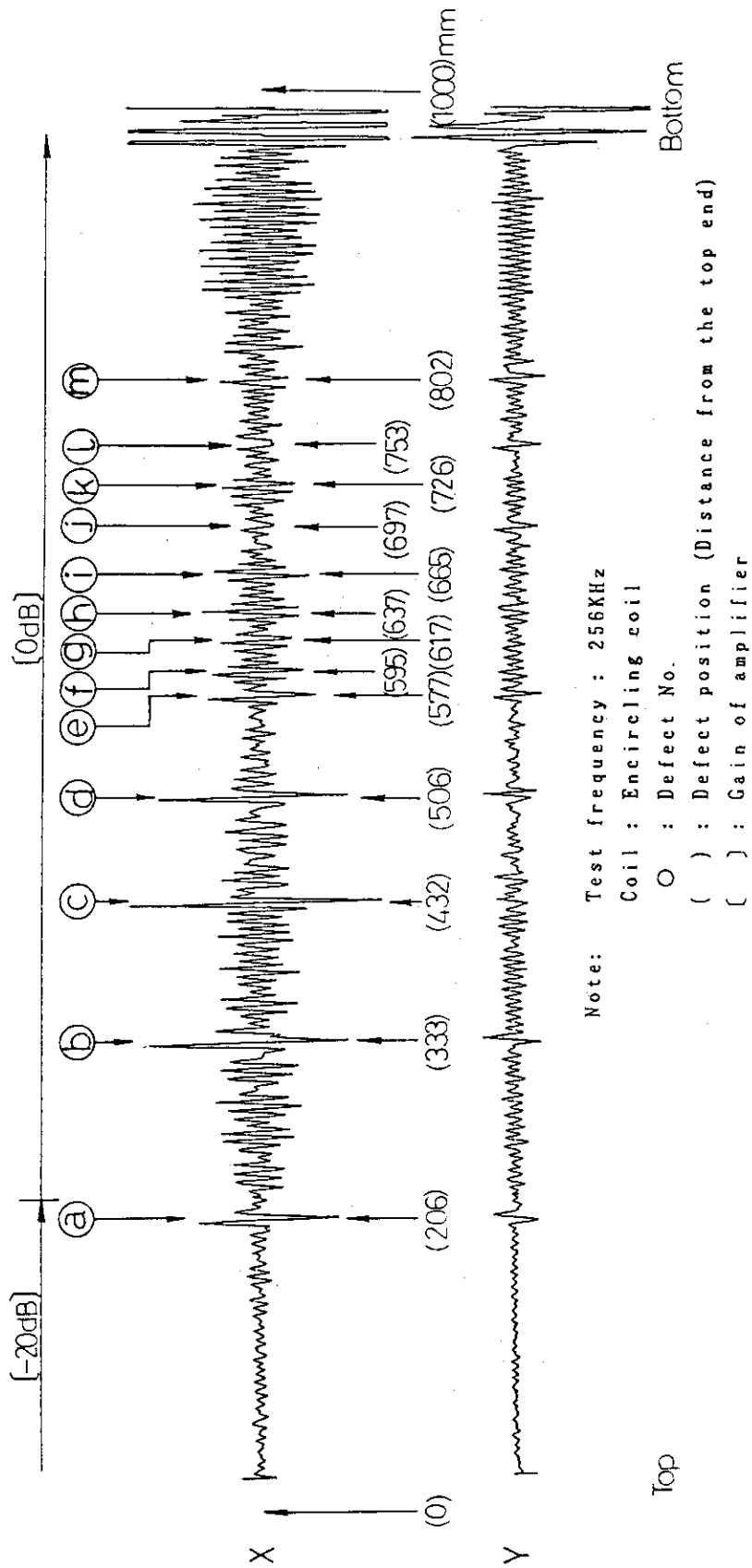


Fig. 13 OUTPUT CHART ON TEST TUBE

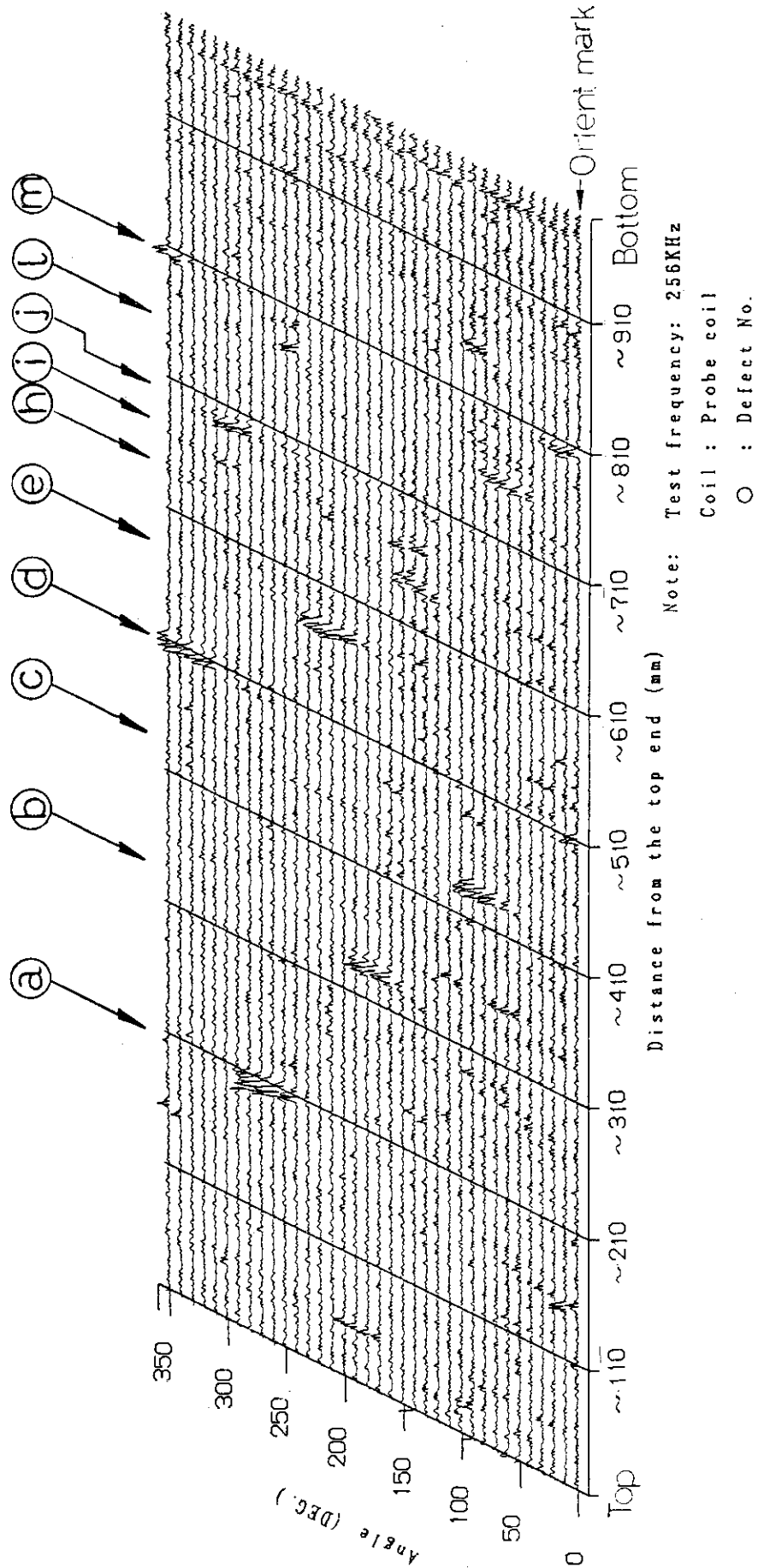
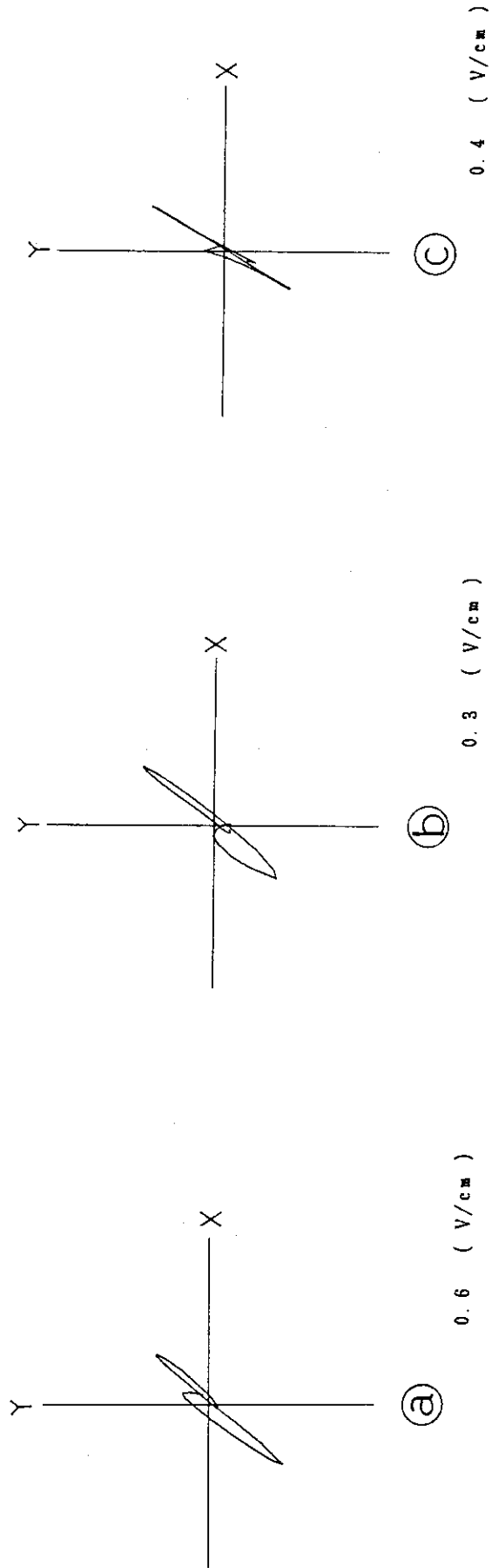
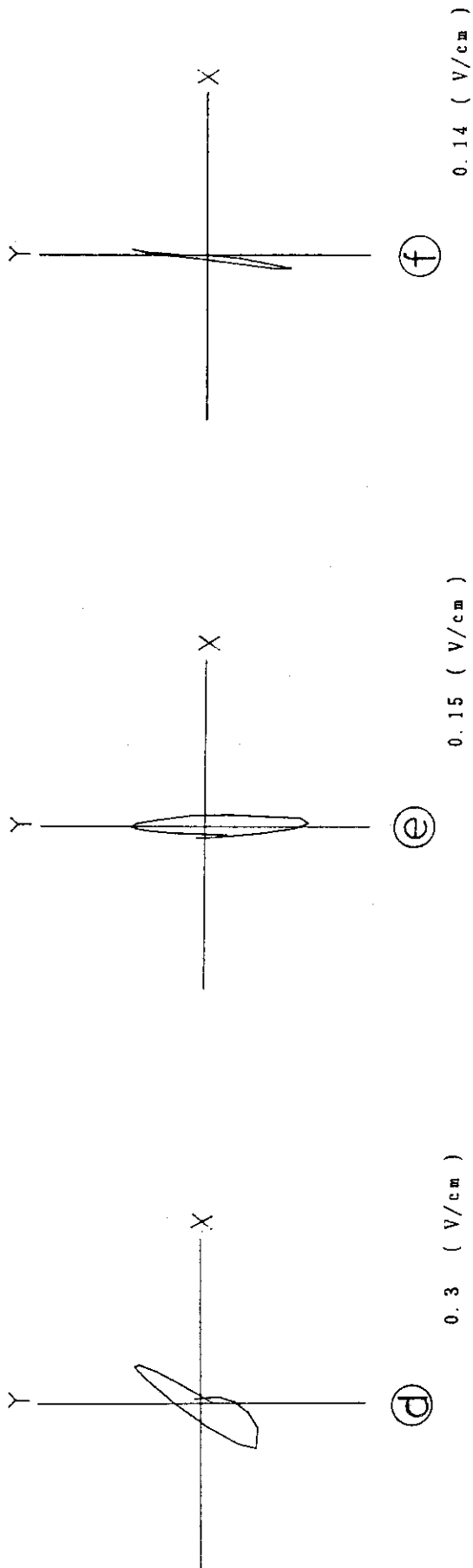


Fig. 14 THREE DIMENSIONAL PLOTS OF SIGNALS FOR TEST TUBE



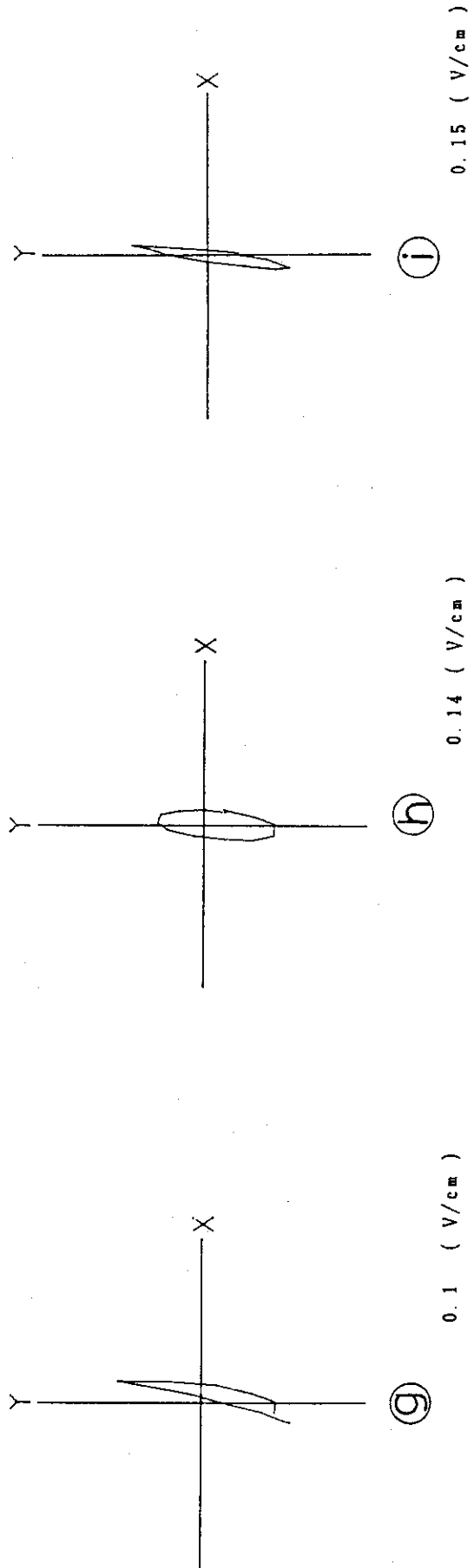
Note: Test frequency: 256KHz
Coil: Encircling coil

Fig. 15 X-Y PLOTS FOR DEFECT No. (a). (b). (c) IN TEST TUBE



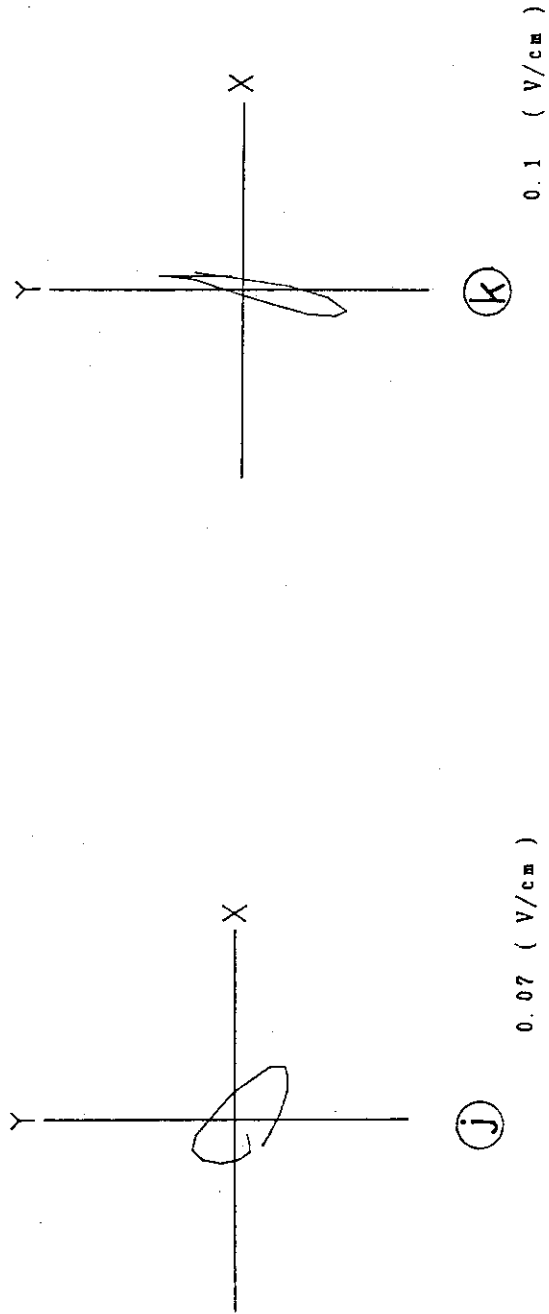
Note: Test frequency: 256KHz
Coil : Encircling coil

Fig. 16 X-Y PLOTS FOR DEFECT No. (d). (e). (f) IN TEST TUBE



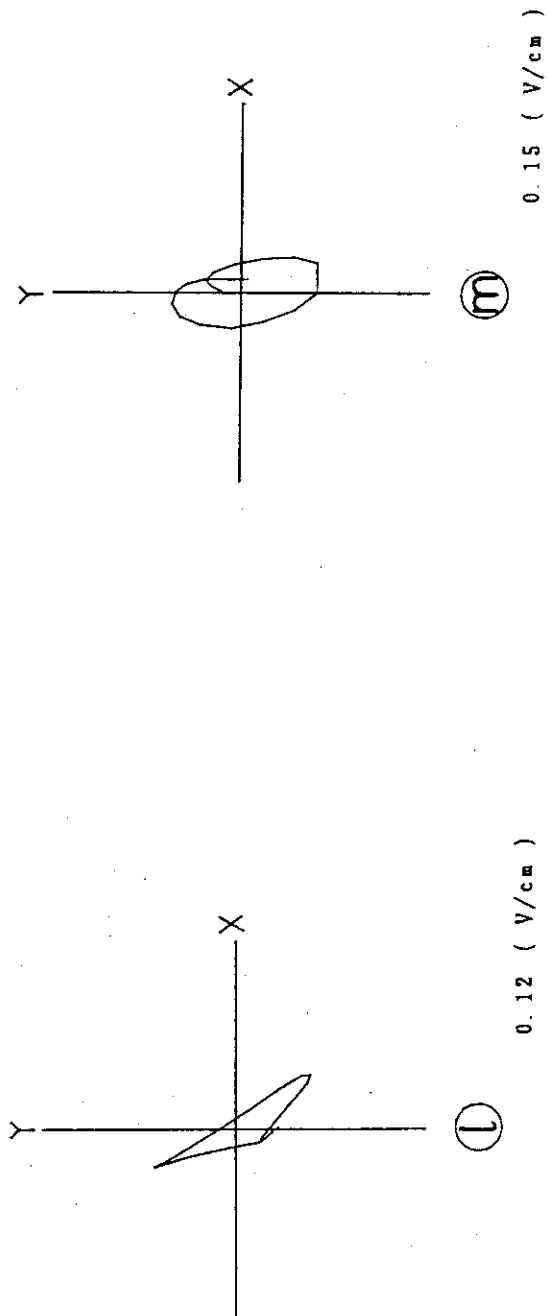
Note: Test frequency: 256KHz
Coil : Encircling coil

Fig. 17 X-Y PLOTS FOR DEFECT No. (g). (h). (i) IN TEST TUBE



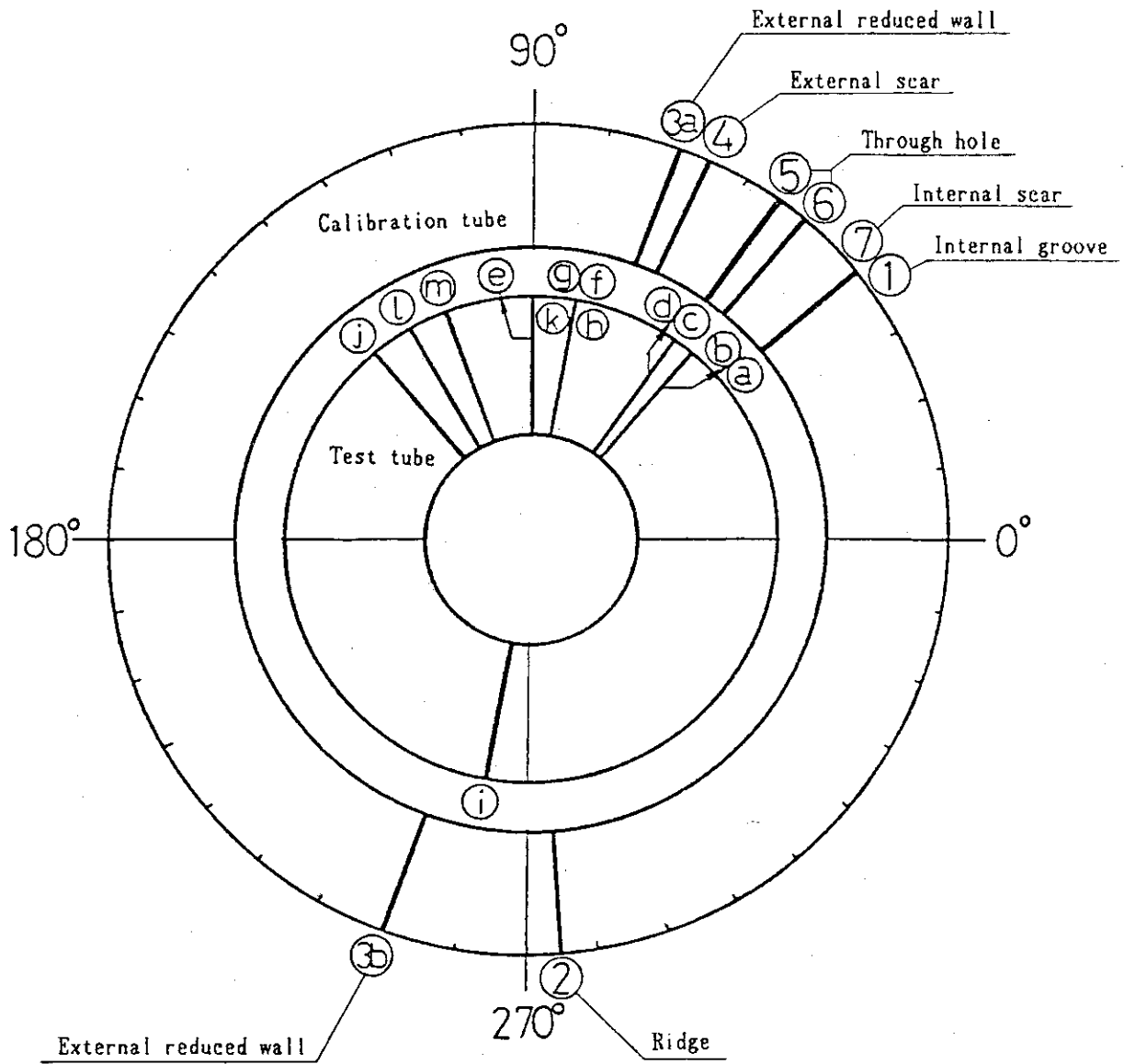
Note: Test frequency: 256KHz
Coil : Encircling coil

Fig. 18 X-Y PLOTS FOR DEFECT No. (j), (k) IN TEST TUBE



Note: Test frequency: 256KHz
Coil : Encircling coil

Fig. 19 X-Y PLOTS FOR DEFECT No. ①, ①, ① IN TEST TUBE



Note: Test frequency : 256KHz
 Coil : Encircling coil
 ○ : Defect No.

Fig. 20 PHASE ANGLE COMPARISON BETWEEN CALIBRATION AND TEST TUBE